Characterization of TAT-Mediated Transport of Detachable Kinase Substrates†

Joseph S. Soughayer,‡,⊥ Yan Wang,‡ Huaina Li,‡ Shing-Hu Cheung,§ Frank M. Rossi,‡,∥ Eric J. Stanbridge,§ Christopher E. Sims,*,‡ and Nancy L. Allbritton*,‡

Department of Physiology and Biophysics and Department of Microbiology and Molecular Genetics, College of Medicine, University of California, Irvine, California 92697

Received December 21, 2003; Revised Manuscript Received April 24, 2004

ABSTRACT: The conjugation of peptides derived from the HIV TAT protein to membrane-impermeant molecules has gained wide acceptance as a means for intracellular delivery. Numerous studies have addressed the mechanism of uptake and kinetics of TAT translocation, but the cytosolic concentrations and bioavailability of the transported cargo have not been well-characterized. The current paper utilizes a microanalytical assay to perform quantitative single-cell measurements of the concentration and accessibility of peptide-based substrates for protein kinase B (PKB) and Ca^{2+}/calmodulin-activated kinase II. The substrate peptide and TAT were conjugated through a releasable linker, either a disulfide or photolabile bond. Free substrate peptide concentrations of $\sim 10^{-20}-10^{-18}$ moles were attainable in a cell when substrates were delivered utilizing these conjugates. The substrate peptides delivered as a disulfide conjugate were often present in the cytosol as several oxidized forms. Brief exposure of cells loaded with the photolabile conjugates to UVA light released free substrate peptide into the cytosol. Substrate peptide delivered by either conjugate was accessible to cytosolic kinase as demonstrated by the efficient phosphorylation of the peptide when the appropriate kinase was active. After incubation of the conjugated substrate with cells, free, kinase-accessible substrate was detectable in less than 30 min. Release of the majority of loaded substrate peptide from sequestered organelles occurred within 1 h. The utility of the photocleavable conjugates was demonstrated by measuring the activation of PKB in 3T3 cells after addition of varying concentrations of platelet-derived growth factor.

Biological membranes form a barrier that prevents the flux of most molecules in to and out of cells (*1*). Nevertheless, the introduction of polar, membrane-impermeant molecules into cells has played an important role in the investigation of cellular behavior (*2*−*6*). Over the past 15 years, short peptide sequences, known as protein transduction domains or PTDs (also known as cell-penetrating peptides), have become increasingly prevalent as tools to internalize otherwise impermeant molecules into cells (*7*). Of the numerous PTDs that have now been discovered, the transduction domain from the HIV TAT protein has been the most widely used and characterized (*8*, *9*). The capacity of this protein to cross biological membranes was first discovered in 1988, when investigators observed that exogenously delivered TAT protein could translocate to the nucleus and activate transcription (*10*, *11*). The ability of the TAT protein to cross the plasma membrane has since been shown to reside primarily in a highly basic region composed of the 9-amino acid residues 49−57 (RKKRRQRRR) (*12*, *13*). Peptides incorporating this sequence have been used to deliver an extensive assortment of biomolecules into cells, ranging from small peptides and peptide nucleic acids to full-length proteins and nanoparticles (*14*−*17*).

The exact mechanism by which TAT enters cells is unknown (*17*). Some investigators have suggested that transduction is mediated by a novel pathway of transport. Studies have shown that PTD entry into cells appears to be receptor-independent and occurs in essentially all cell types (*15*, *18*). Investigators have demonstrated efficient intracellular uptake of the TAT(48−60) peptide at 4 °C, suggesting that uptake occurred by a process other than endocytosis (*19*, *20*). Suzuki and co-workers utilized a variety of pharmacologic inhibitors to block active cellular uptake processes such as endocytosis with little effect on internalization of TAT(48−60) (*21*). However, it is now clear that because of the high avidity of TAT for the plasma membrane TAT conjugates bound to the cell at low temperatures remain there even after washing. This bound conjugate can then be taken up when the cells are rewarmed for analysis unless special wash steps are undertaken (*14*). Two recent studies have utilized trypsin wash steps to remove bound TAT conjugates from the cell exterior before analysis (*14*, *22*). A study by Fittapldi et al. provided strong evidence for the role of lipid rafts and caveolar endocytosis for TAT-mediated uptake (*22*). Likewise, Richard and co-workers demonstrated that cellular uptake of both TAT(48−60) and a related peptide, $(Arg)_9$, was inhibited by low temperatures or ATP depletion (*14*). These studies also suggested that transport

† This work was supported by National Institutes of Health Grants GM57015 and NS/MH39310 to N.L.A.

* To whom correspondence should be addressed. Tel.: 949-824-6493. Fax: 949-824-8540. E-mail: nlallbri@uci.edu (N.L.A.); cesims@uci.edu (C.E.S.).

‡ Department of Physiology and Biophysics.

§ Department of Microbiology and Molecular Genetics.

∥ Current address: Cell Biosciences, Inc., 1050 Page Mill Road, Palo Alto, CA 94303.

⊥ Current address: Vollum Institute, 3181 SW Sam Jackson Park Road, L474 Portland, OR 97239.

10.1021/bi036296d CCC: $27.50
Published on Web 06/08/2004

may take much longer than once thought. Whereas earlier data indicated that loading took less than 1 min, these new data reported that up to 10 h were required to achieve complete loading of a recombinant TAT(48−58) green fluorescent protein (GFP) (*22*). Most recently, work by Potocky and co-workers suggests that TAT release into the cytosol requires an acidified, endocytic compartment (*23*).

Intracellular TAT−cargo concentrations are reported to be over 100 times greater than that added to the extracellular environment, suggesting that cells are capable of not only taking in the TAT−cargo, but also of greatly concentrating the TAT−cargo with respect to the extracellular solution (*9*, *24*). However, the quantity of TAT−cargo released into the cytosol (as opposed to remaining inside organelles) and the accessibility of the cargo to cytosolic molecules has not yet been characterized. Much of the intracellular TAT−cargo may be sequestered within inaccessible compartments rather than free within the cyosol. In the majority of studies to date, the TAT peptide and cargo have been covalently linked. In this case, the intracellular fate and biological activity or accessibility of the cargo may also be heavily influenced by the TAT sequence and vice versa (*3*, *25*, *26*). Investigators studying the inhibition of kinase activity using small inhibitory peptides have shown that the addition of a TAT sequence was deleterious to the bioactivity of the peptide in vitro and in vivo (*25*). Stein et al. showed that the intracellular bioactivity of an anti-tetanus $F(ab')_2$ fragment was retained only when transported into cells conjugated to a TAT peptide via a cleavable disulfide bond (*3*). The same cargo linked to the TAT peptide by a peptide bond failed to exhibit activity. Although these studies did not determine the mechanism for these differences in activity, it is clear that the TAT sequence can alter the behavior of the cargo. Studies examining the cytosolic concentrations and the fate of cargo released from the TAT sequence once inside the cell would provide important insight into the bioavailability and physiological effects of the cargo molecules.

Studies on the uptake of TAT conjugates have typically used fluorescence microscopy or flow cytometry to follow the cellular uptake of a fluorescently labeled species (*19*−*21*, *24*, *25*). Frequently, extracellular TAT concentrations above 5 μM have been required to achieve adequate intracellular concentrations of a fluoresecently tagged molecule for its visualization. Loading cells with these high extracellular TAT concentrations can be toxic (*19*, *24*). In addition, the mechanism(s) and efficiency of TAT entry into cells may be difficult to identify if one or more steps are saturable at low TAT concentrations. The ability to study TAT translocation into cells at low extracellular and cytosolic concentrations would be valuable in experiments to determine the fate of the cargo and potentially the mechanism of TAT translocation.

In the present paper, we have utilized a microanalytical instrument to provide quantitative data on cargo transported into the cytoplasm of living cells (*27*−*30*). Fluorescently labeled peptides, which were substrates for kinases, were conjugated to a TAT-derived peptide. Two strategies were employed to introduce a cleavage site between the TAT and the substrate cargo, a disulfide bond and a photolabile moiety. Cytosolic concentrations of the released substrates were detectable at approximate concentrations of less than 10 nM (10^{-20} moles in a cell of 1 pL). These substrate peptides were used as probes of cytoplasmic kinase activity in single cells, with their phosphorylation providing a measure of their accessibility to cytoplasmic kinases. The percentage of phosphorylation of a TAT-loaded substrate peptide was compared to that achieved with microinjection to determine whether the free peptide released from the TAT conjugate was efficiently phosphorylated. The conjugated peptides were also used to determine the kinetics and temperature dependence of TAT-mediated delivery of kinase-accessible peptide to the cytosol.

EXPERIMENTAL PROCEDURES

Materials. Tissue culture reagents were purchased from Invitrogen (Grand Island, NY). [^{32}P]-γATP was purchased from NEN (Boston, MA). Extracellular buffer (ECB)[1] was composed of 135 mM NaCl, 5 mM KCl, 10 mM HEPES (pH 7.4), 1 mM $MgCl_2$, and 1 mM $CaCl_2$. Capillaries were purchased from Polymicro Technologies (Phoenix, AZ). Bovine serum albumin (BSA) was purchased from Sigma−Aldrich (St. Louis, MO). *N*-Succinimidyl 3-[2-pyridyldithio]-propionamido (SPDP) was obtained from Molecular Biosciences, Inc. (Boulder, CO). Recombinant calcium−calmodulin-activated kinase II (CamKII) and calmodulin were purchased from Calbiochem (San Diego, CA). D-*myo*-Phosphatidylinositol 3,4,5-trisphosphate and D(+)-*sn*-1,2-di-*o*-hexadecanoylglyceryl, 3-*O*-phospho linked (DiC_{16}PtdIns-[3,4,5]P_3) and histone H1 were a kind gift from Echelon (Salt Lake City, UT). Platelet-derived growth factor BB (PDGF-BB) was from Upstate Biotechnology (Lake Placid, NY). Cell lysis buffer, rabbit anti-total Akt/PKB antibody, rabbit anti-phospho Akt/PKB (Ser473) antibody, and mouse anti-phospho p38 MAPK (Thr180/Tyr182) antibody were obtained from Cell Signaling Technology (Beverly, MA). A BCA protein assay kit and "SuperSignal Chemiluminiscent Substrate" were purchased from Pierce Chemical Company (Rockford, IL). Immobilon-P membranes were bought from Millipore (Billerica, MA), while horseradish peroxidase-conjugated anti-rabbit antibody and horseradish peroxidase-conjugated anti-mouse antibody were from Santa Cruz Biotechnology (Santa Cruz, CA). All other reagents were purchased from Fisher Scientific (Pittsburgh, PA).

Source of Peptides and Peptide Components. Fmoc-protected amino acids and the Fmoc-aminoethyl photolabile linker (4-[4-(1-(F_{moc}amino)ethyl)-2-methoxy-5-nitrophenoxy]-

[1] Abbreviations: PTD, protein transduction domain; ECB, extracellular buffer; BSA, bovine serum albumin; FCS, fetal calf serum; SPDP, *N*-succinimidyl 3-[2-pyridyldithio]propionamido; PLL, photolabile linker; SS, disulfide linker; CamKII, calcium−calmodulin-activated kinase II; PKB, protein kinase B; F−PKB−C, fluorescein−GRPRAATFAEGC; F−PKB, fluorescein−GRPRAATFAEG; TAT(49−57), RKKRRQRRR; F−CamKII−TAT, fluorescein−KKALHRQETVDAL−RKKRRQRRR; F−CamKII, fluorescein−KKALHRQETVDAL; F−CamKII−C, fluorescein−KKALHRQETVDALC; F−PKB−PLL−TAT, fluorescein−GRPRAATFAEG−(PLL)−RKKRRQRRR; F−PKB−C−SS−TAT, fluorescein−GRPRAATFAEGC−(SS)−RKKRRQRRR; F−CamKII−PLL−TAT, fluorescein−KKALHRQETVDAL−(PLL)−RKKRRQRRR; F−CamKII−C−SS−TAT, fluorescein−KKALHRQETVDALC−(SS)−RKKRRQRRR; RBL, rat basophilic leukemia; CE, capillary electrophoresis; LMS, Laser Micropipet System; CACE, Cell Activity by Capillary Electrophoresis; PI3K, phosphatidylinositol 3-kinase; PIP_3, phosphatidylinositol 3,4,5-trisphosphate; DiC_{16}PtdIns-[3,4,5]P_3), D-*myo*-phosphatidylinositol 3,4,5-trisphosphate and D(+)-*sn*-1,2-di-*o*-hexadecanoylglyceryl, 3-*O*-phospho linked; DTT, dithiothreitol.

butanoic acid) were purchased from Novabiochem (Switzerland). The following peptides were synthesized at the Beckman Peptide and Nucleic Acid Facility at Stanford University with amidated C termini, then fluorescently labeled, and purified as described below. The peptides were F−PKB−C (fluorescein−GRPRAATFAEGC), F−PKB (fluorescein−GRPRAATFAEG), TAT(49−57) (RKKRRQRRR), F−CamKII−TAT (fluorescein−KKALHRQETVDAL−RKKRRQRRR), F−CamKII (fluorescein−KKALHRQETVDAL), and F−CamKII−C (fluorescein−KKALHRQETVDALC). The phosphorylated forms (with phosphates on the underlined residues) were also synthesized at the Beckman Peptide and Nucleic Acid Facility with amidated C termini, then fluorescently labeled, and purified. F−CamKII, a substrate for CamKII, was derived from the threonine 286 autophosphorylation site on CamKII (*31*). F−PKB, a substrate for protein kinase B (PKB), was based on the substrate RPRAATF as originally described by Alessi et al. (*30*, *32*).

F−PKB−PLL−TAT (fluorescein−GRPRAATFAEG−(PLL)−RKKRRQRRR) and F−PKB−C−SS−TAT (fluorescein−GRPRAATFAEGC−(SS)−RKKRRQRRR) were synthesized and purified "in house" as described below. "-(PLL)-" represents a photolabile linker, while "-(SS)-" denotes a disulfide-bond linkage between the peptides. F−CamKII−PLL−TAT (fluorescein−KKALHRQETVDAL−(PLL)−RKKRRQRRR) and F−CamKII−C−SS−TAT (fluorescein−KKALHRQETVDALC−(SS)−RKKRRQRRR) were synthesized and purified at Anaspec (San Jose, CA).

Cell Culture. NIH 3T3, HT1080, and rat basophilic leukemia (RBL-2H3) cells were grown in Dulbecco's modified eagle media (DMEM) supplemented with 10% fetal calf serum (FCS), 4 mM L-glutamine, penicillin (100 units/mL), and streptomycin (100 μg/mL) at 37 °C in 5% CO_2. HT1080/PTEN cells were maintained in the same medium with the addition of a selective antibiotic (800 μg/mL of Geneticin). Cells used in experiments were grown in a cell chamber made by using Sylgard 184 (Dow Corning, Midland, MI) to attach a Teflon "O" ring ($^{15}/_{16}$ in outer diameter) to a 25-mm, round, #1 glass coverslip. In some instances, the coverslips were coated with collagen to increase cellular adherence to the glass surface. Cells were plated at a density of 5−10 cells per high power field. Prior to use, the cells were allowed to grow in supplemented media for 12−24 h after plating in the cell chamber. HT1080 and RBL cells were then serum-starved with DMEM containing 0.25% FCS for 18 h prior to experiments. 3T3 cells were serum-starved with DMEM without FCS for 18 h prior to experiments. Experiments with cells were conducted at 37 °C unless otherwise stated.

Labeling Peptides with Fluorescein. Peptides were labeled with fluorescein on the amino terminus and deprotected as described previously (*29*).

Peptide Purification and Characterization. Peptides were purified by HPLC as described previously (*27*). The molecular weight and peptide purity were assessed by MALDI-MS (PE Biosystems Voyager System 4124) and capillary electrophoresis (CE), respectively. The concentration of the fluorescein-labeled peptide was determined by amino acid analysis at the Molecular Structure Facility at the University of California, Davis by adding to the sample a standard of known concentration.

Peptide Conjugation through a Disulfide Bond. TAT(49−57) attached to the synthetic resin was modified on its amino terminus with 50 μmol of the heterobifunctional cross-linker SPDP [or a 1:5 molar ratio (TAT(49−57)/SPDP)] in 256 μL of dichloromethane and in the presence of 1.2 equiv of diisopropylethylamine for 2 h. The pyridyldithiol group preferentially reacts with free sulfhydryls, limiting the generation of disulfide-linked TAT(49−57) homodimers (*33*). The peptide was cleaved in 95% trifluoroacetic acid (v/v), 2.5% water (v/v), and 2.5% anisole (v/v), ether precipitated, and dissolved in a minimal volume of triethylammonium acetate (100 mM at pH 7). The SPDP-reacted TAT(49−57) peptide was added at an estimated molar ratio of 1:1 to the fluorescein-labeled substrate containing a cysteine on the carboxy terminus. The mixture was incubated at room temperature for 2 h. The disulfide-linked peptide F−PKB−C−SS−TAT or F−CamKII−C−SS−TAT was isolated and characterized as described above.

Peptide Conjugation through a Photolabile Linker. The Fmoc-aminoethyl photolabile linker was added to the amino terminus of resin-bound TAT(49−57) using standard Fmoc (*N*-(9-fluorenyl)methoxycarbonyl) chemistry at 0.1 mmol scale on an ABI model 433A peptide synthesizer (Foster City, CA). The PKB substrate peptide (GRPRAATFAEG) was then added to the photolabile linker using the synthesizer. Fluorescein was added to the amino terminus of the resin-bound peptide, and the peptide was deprotected and purified.

In Vitro Kinase Assay. Peptides (5−60 μM) were phosphorylated in vitro by recombinant CamKII (100 units as defined by the manufacturer, Calbiochem) in 20 mM Tris-HCl, 10 mM $MgCl_2$, 0.5 mM dithiothreitol (DTT), and 0.1 mM EDTA at pH 7.5 with 2.4 mM calmodulin, 2 mM $CaCl_2$, and 100 mM [^{32}P]-γATP. The final specific activity of the [^{32}P]-γATP was 100 cpm/pmol, and the total reaction volume was 25 μL. The mixture was incubated at 30 °C for 30 min. Reactions were stopped with the addition of ice-cold 10% (v/v) trichloroacetic acid (45 μL), vortexed, centrifuged, and blotted onto P81 phosphocellulose paper. Phosphate incorporation was quantified with a liquid scintillation counter (Beckman Instruments LS 3801, Irvine, CA).

Laser Micropipet System (LMS)/Cell Activity by Capillary Electrophoresis (CACE). The LMS has been previously described (*27*−*29*). This system is also called CACE, which parallels the naming of other technologies utilizing chemical separations. Briefly, cells were placed on an inverted fluorescence microscope stage (Diaphot 300, Nikon, Japan) and maintained at 37 °C with an objective heater (Bioptechs, Butler, PA) prior to lysis unless stated otherwise. The cells were continually washed with ECB maintained at 37 °C (unless stated otherwise) with a flow rate of 1 mL/min and a total chamber volume of 0.5 mL. The inlet of a capillary (30 μm inside diameter, 360 μm outside diameter, and 75 cm long) was positioned 10 μm above the cell. The inverted microscope was coupled to a pulsed Nd/YAG laser and a CE system (*29*). The LMS/CACE-based assay was performed as previously described (*27*, *34*). Cells were always maintained in ECB when analyzed with the LMS/CACE.

With the LMS/CACE, a cell can be rapidly lysed and the cellular contents loaded with nearly 100% efficiency into a capillary in well under 33 ms (*27*, *29*, *34*). Simultaneously with cell lysis, electrophoretic separation of the contents of the cell is initiated. The fast lysis coupled with turbulent

mixing and electrophoretic separation terminates the cellular reactions in under 33 ms (*27*, *34*). Until the moment of lysis, the cell is undisturbed and resides in a physiologic buffer solution (ECB). Phosphorylated and nonphosphorylated forms of a kinase-substrate peptide are separated by CE and detected by laser-induced fluorescence to provide a "snapshot" of the activity of the measured kinase(s) at the moment of cell lysis. Because the peptides can be dephosphorylated, the method measures the balance between the kinases and phosphatases acting on the peptide (*30*).

CE. CE was performed as described previously with the following exceptions (*29*). The inner walls of the capillaries (30 μm inside diameter and 360 μm outside diameter) were coated with poly(acrylate) (*35*). The outlet of the capillary was held at a negative potential of 18−21 kV, and the inlet reservoir was held at ground potential. Under these conditions, the current through the capillary was typically ∼36 μA. Solutions of standards were loaded into the capillary by gravitational fluid flow. The volume loaded was calculated from Poiseulle's equation and from contributions by spontaneous fluid displacement and diffusion (*36*−*38*). To estimate the number of moles of peptide in an unknown solution or within a cell, the peak area from the electrophoretic trace of the solution or the cell was compared to that of a standard of known concentration electrophoresed on the same day. A 1-pL cell volume and 100% peptide recovery were assumed in calculating the cytosolic peptide concentration (*27*, *29*). Analytes were detected by laser-induced fluorescence (*29*).

Cleavage of the Photolabile Peptides. The photolabile TAT(49−57) conjugate (1 nM or 10 μM in ECB) was illuminated with UVA (20 mW/cm^2 at 2 in from the lamp) using a 365-nm light source (UVP Blak-Ray B100AP, Upland, CA) for the times specified in the results section. The emission maxima for the photolabile group was 365 nm. After photorelease, the concentration of the fluorescent substrate was electrophoresed and quantitated by CE.

Construction of the Standard Curve for Photolabile Peptides. A known concentration of the photocleavable reporter was placed in an uncapped, shallow vial. The sample was then illuminated with the UVA light source for varying times as described above. A small amount of the sample was then removed, and the amount of released peptide was quantitated using CE. The amount of released substrate was plotted, and the linear portion of the curve was then fitted to a straight line using a linear regression algorithm (Origin, Origin Lab Corp., North Hampton, MA). The slope represented the rate of photocleavage.

Loading Cells with TAT(49−57) Conjugated Substrates. Cells were incubated at room temperature for 5 min in 1% BSA in ECB, washed in ECB, and then incubated for 5 min at room temperature (unless stated otherwise) at the stated concentration with either a substrate conjugated to TAT(49−57) through a peptide bond, a substrate−PLL−TAT(49−57) conjugate, or a substrate−SS−TAT(49−57) conjugate. The cells were then washed again with 1% BSA in ECB. Cells loaded with the disulfide conjugate were placed in DMEM supplemented with 10% FCS, 4 mM L-glutamine, penicillin (100 units/mL), and streptomycin (100 μg/mL) and incubated at 37 °C in 5% CO_2 for 20 min (unless stated otherwise). Cells loaded with the photolabile conjugate were placed in supplemented DMEM and incubated at 37 °C in 5% CO_2 for 10 min (unless stated otherwise) and were then illuminated with the UVA light source for 10 s (a radiant energy/unit area of 1 kJ/m^2). The supplemented DMEM was exchanged, and the cells were incubated another 10 min at 37 °C in 5% CO_2 (unless stated otherwise). Just prior to analysis, the cells were washed into ECB.

Addition of Phosphatidylinositol 3,4,5-Trisphosphate (PIP_3) to Cells. Long-chain synthetic phospholipids [DiC_{16}PtdIns (3,4,5)P_3 sodium salt] or PIP_3 were freshly prepared at 300 μM in 150 mM NaCl, 4 mM KCl, and 20 mM HEPES at pH 7.2 and resuspended by bath sonication or vigorous vortexing (*39*). Histone−phospholipid complexes were prepared by combining 300 μM phospholipids with 100 μM freshly prepared histone. The mixture was vortexed and then incubated for 5 min at room temperature. The solution was diluted 1:10 with ECB immediately before addition to the cells on the coverslips. Cells were incubated with the histone−phospholipid complexes for 10 min at 37 °C before analysis with the LMS/CACE.

Stimulation of NIH-3T3 Cells with PDGF. A total of 10 μg of PDGF-BB was rehydrated in 1 mL of 10 mM acetic acid containing 2 mg/mL BSA. An aliquot was stored at −20 °C until use. Stock PDGF-BB (10 μg/mL) was diluted to the desired final concentration in a dish of subconfluent cells that were starved in serum-free DMEM. Cells were incubated at 37 °C for 10 min.

Measurement of p38 Kinase and PKB Activation in Response to Exposure to UVA Light. A dish of subconfluent cells was washed with ECB. The cells were then exposed to UVA light for varying times under conditions identical to that used for photocleavge and then allowed to recover in serum-free DMEM for 15 min at 37 °C. Cells were washed once with PBS and then processed for Western blotting as described below.

Measurement of p38 Kinase and PKB Activation by Western Blot. Cells were scraped into 350 μL of 1× cell lysis buffer with 1% phenylmethylsulfonyl fluoride and shaken on ice for 20 min. The cell lysate was centrifuged at 13000*g* for 7 min at 4 °C. The protein concentration of the resulting supernatant was measured with a BCA protein assay kit. Samples, each containing 50 μg of protein, were electrophoresed by SDS−10% polyacrylamide gel electrophoresis (PAGE) and transferred to Immobilon-P membranes. The membrane was blocked in ST buffer (20 mM Tris at pH 7.5, 150 mM NaCl, and 0.1% Tween 20) containing 5% nonfat milk for 1 h at room temperature. Membranes were then probed with the relevant antibodies. Rabbit anti-phospho Akt/PKB and mouse anti-phospho p38 MAPK antibodies were incubated with the membranes at 4 °C overnight. The membranes were also incubated with an antibody against β actin, which was used as a marker for total protein loaded. The membranes were washed for 5 min for three times with ST buffer at room temperature. The membranes were then incubated with horseradish peroxidase-conjugated anti-rabbit antibody (1:10000) or horseradish peroxidase-conjugated anti-mouse antibody (1:5000) for 1 h at room temperature. The membranes were then washed three times, each time for 5 min with fresh ST buffer at room temperature. The immune complexes were detected with SuperSignal Chemiluminescent Substrate.

RESULTS

Characterization of TAT(49−57) Conjugated to a Substrate Peptide. To determine whether a kinase substrate linked to TAT(49−57) was accessible to cytosolic enzymes, we incubated RBL cells with 1 μM F−CamKII conjugated to TAT(49−57) (F−CamKII−TAT) through a peptide bond. To determine whether the F−CamKII−TAT might be accessible to the kinase of interest (CamKII), cells were loaded with F−CamKII−TAT and then their contents were analyzed with the LMS/CACE. When single cells were analyzed with the LMS/CACE, no fluorescent peaks at the detection wavelengths (excitation, 488 nm; emission, 505−565 nm) were observable on the electrophoretic trace within 6000 s, the longest time measured. When F−CamKII without the conjugated TAT(49−57) was loaded into cells by microinjection and the cell was analyzed using the LMS/CACE, F−CamKII possessed a migration time of 800 s and a detection limit of 3×10^{-21} mol. Because F−CamKII−TAT has a higher net positive charge-to-mass ratio than the unconjugated F−CamKII, F−CamKII−TAT would be expected to have an electrophoretic migration time much shorter than 800 s. To determine whether the TAT(49−57) sequence might be causing anomalous electrophoretic behavior of F−CamKII−TAT, we loaded standard solutions of either fluorescein−TAT(49−57) or F−CamKII−TAT into a capillary and initiated electrophoresis. Neither peptide eluted from the capillary within 6000 s even when 10^{-17} mol was loaded into the capillary. When the F−CamKII−TAT was placed on a glass surface similar to the fused-silica inner walls of the capillary, the peptide was seen to strongly adsorb to the glass surface (data not shown). Thus, the most likely explanation for the absence of a detectable fluorescent peak during electrophoresis was the adsorption of the highly positive TAT(49−57) sequence to the negatively charged glass wall of the capillary.

In addition to assessing the electrophoretic behavior of F−CamKII−TAT, the ability of this conjugated sequence to act as an efficient substrate for CamKII was characterized. The amount of phosphate incorporated into the substrate peptide alone and into F−CamKII−TAT by CamKII was measured in vitro. In this range of peptide concentrations measured, 90% less phosphate was incorporated by the kinase into F−CamKII−TAT compared to the peptide lacking TAT(49−57). The kinetic properties of CamKII for this substrate peptide were degraded when the peptide was conjugated to TAT(49−57).

Characterization of Substrate Peptides Conjugated to TAT-(49−57) by a Disulfide Bond. Previous investigators developed cleavable PTD−cargo conjugates by engineering a disulfide linkage between the two domains (*3*, *24*). In the oxidative extracellular environment, the disulfide bond remained intact, but in the reductive cytosolic environment, the disulfide bond quickly reduced releasing the cargo from the PTD (*24*, *40*). TAT(49−57) was conjugated via a disulfide bond to cysteines added to substrate peptides for CamKII or PKB, denoted F−CamKII−C−SS−TAT and F−PKB−C−SS−TAT, respectively. The TAT(49−57)-conjugated substrates were incubated with cells (HT1080 or HT1080/PTEN), and the contents of the cells were analyzed by the LMS/CACE. HT1080 cells have constitutive PKB activity because of a mutated allele of the *N-ras* gene, resulting in the subsequent activation of signaling proteins downstream of the ras protein (*41*). A second cell line, HT1080/PTEN, has been engineered to overexpress wild-type PTEN, a lipid phosphatase, which metabolizes PIP_3, resulting in greatly diminished PKB activity in the HT1080/PTEN cells (*42*). HT1080 cells do not have constitutive CamKII activity (data not shown).

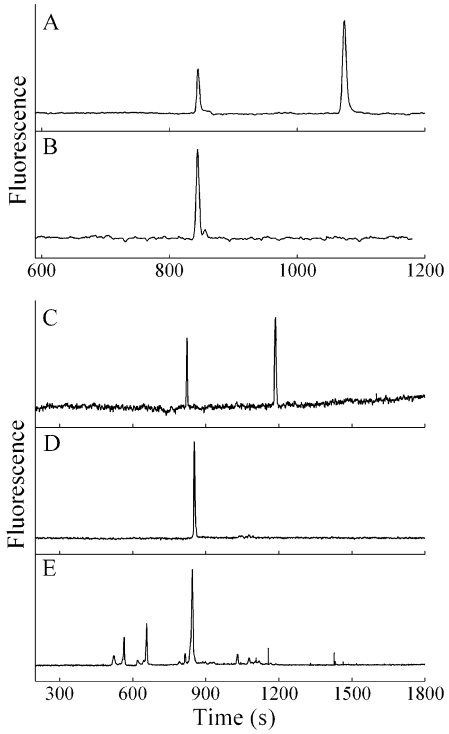

FIGURE 1: Electrophoretic analysis of single cells loaded with peptide substrates conjugated to TAT(49−57) through a disulfide bond. (A) Electrophoretic trace of a mixture of F−CamKII (9×10^{-20} mol) and phosphorylated F−CamKII (5×10^{-19} mol) in buffer solution. (B) HT1080 cell loaded with the disulfide conjugate F−CamKII−C−SS−TAT. A typical electrophoretic trace from a single-cell analysis is shown. (C) Electrophoretic trace of a mixture of F−PKB (8×10^{-20} mol) and phosphorylated F−PKB (1×10^{-19} mol) in buffer solution. (D) Electrophoretic trace of an HT1080/PTEN cell loaded with the disulfide conjugate F−PKB−C−SS−TAT at an extracellular concentration of 1 μM. (E) Electrophoretic trace of an HT1080/PTEN cell loaded as in D but demonstrating a multitude of unidentified peaks (see text).

Electrophoretic traces of the contents of all HT1080 cells loaded with F−CamKII−C−SS−TAT (at an extracellular concentration of 750 nM) demonstrated a single major peak with a migration time identical to that of a standard of F−CamKII−C ($n > 12$) (parts A and B of Figure 1). Thus, the disulfide bond between the F−CamKII−C and TAT-(49−57) was successfully reduced upon entry into the cells releasing the substrate cargo. As expected, F−CamKII−C showed little to no phosphorylation in the HT1080 cells because no peaks or only very small peaks appeared at the migration time for the phosphorylated form of the peptide.

In contrast, electrophoretic traces from HT1080/PTEN cells loaded with F−PKB−C−SS−TAT (1 μM extracellular concentration) demonstrated a single peak in only 30% of the cells analyzed ($n = 19$). For this subpopulation of cells, the migration time of the single peak was identical to that of a standard of F−PKB−C (parts C and D of Figure 1). As expected, no peak was present that migrated at the time of the phosphorylated form of F−PKB−C in cells, because

PKB has little to no activity in the HT1080/PTEN cells (*30*). In the remaining 70% of the cells, multiple peaks were present on the electrophoretic trace. One of the major peaks possessed a migration time identical to that of a standard of F−PKB−C (Figure 1E). Of the other peaks, none possessed a migration time consistent with phosphorylated F−PKB−C. Because the adsorption of TAT(49−57) to the capillary surface prevented migration through the capillary, the additional peaks could not be F−PKB−C still conjugated to TAT(49−57). It was hypothesized that these peaks were the result of oxidative reactions of the sulfhydryl group present on the F−PKB−C peptide. To determine whether the unidentified peaks could be converted to F−PKB−C by reduction of the sulfhydryl, HT1080/PTEN cells were loaded with F−PKB−C−SS−TAT as above and the reducing agent DTT (1 μM) was added to the solution surrounding the cells just prior to lysis and analysis by the LMS/CACE. DTT was also added to the electrophoretic buffer contained in the capillary. Whenever DTT was present, a single peak with a migration time identical to that of F−PKB−C was present on the electrophoretic trace (data not shown). These data suggest that the additional peaks arose from cytosolic reactions of the sulfhydryl group on the peptide.

Phosphorylation of Substrate Peptides Delivered by a Disulfide-Linked TAT(49−57). To determine whether the detached substrates were in the cytosol and accessible to kinases, the cytosolic phosphorylation of the translocated cargo was studied. In the initial experiment, F−CamKII−C−SS−TAT (750 nM extracellular concentration) was loaded into HT1080 cells. The cells were incubated with ionomycin (500 nM) for 15 min to increase the cytosolic concentration of free Ca^{2+} and activate CamKII (*43*). The electrophoretic traces from these cells displayed a second peak in addition to the peak of the nonphosphorylated F−CamKII−C (data not shown). The migration time of the second peak was identical to that of phosphorylated F−CamKII−C loaded into cells. A total of 52 ± 7% (mean ± standard deviation) (n = 5) of the F−CamKII−C was phosphorylated as determined by comparison of the peak areas. At least half of the F−CamKII−C was in the cytosol and accessible to the kinase. For these cells, the average number of moles per cell was $1.0 \pm 0.4 \times 10^{-19}$, which is equivalent to a cytosolic concentration of ∼100 nM.

Because the properties of F−PKB microinjected into HT1080 cells have been well-characterized, experiments were undertaken to compare the fate of F−PKB−C loaded as F−PKB−C−SS−TAT into HT1080 cells to that of the microinjected F−PKB (*30*). When microinjected, the percentage of phosphorylated F−PKB depended on the relative, steady-state levels of both the kinases and phosphatases (*30*). At total concentrations of F−PKB below the K_M of PKB and the known K_M values of the phosphatases for their substrates, the percent of phosphorylated F−PKB was independent of the total concentration of peptide. In HT1080 cells, approximately 70% of the peptide was phosphorylated at steady state, which was achieved in less than 2 min. In addition, all of the peptide loaded by microinjection was shown to be accessible to PKB for phosphorylation (*30*). When HT1080 cells were incubated with F−PKB−C−SS−TAT (1 μM), 85% (n = 85) of the electrophoretic traces possessed multiple peaks with migration times other than that of nonphosphorylated and phosphorylated F−PKB−C

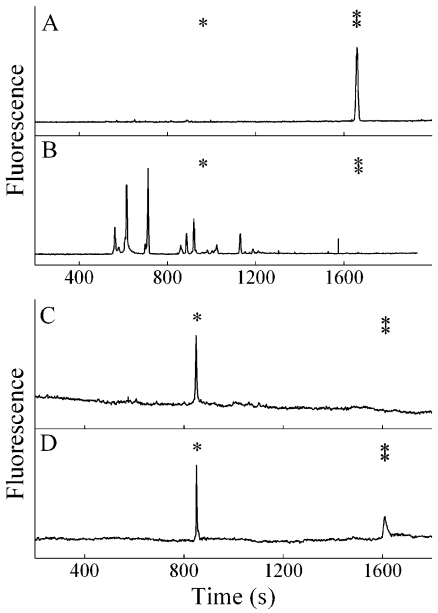

FIGURE 2: Analysis of phosphorylation of the PKB substrate in HT1080 and RBL cells. Electrophoretic traces from cells loaded with F−PKB−C−SS−TAT (1 μM). A single asterisk denotes the migration time of F−PKB, and a double asterisk denotes the migration time of phosphorylated F−PKB from cells on the day of the experiment. (A) Electrophoretic trace from the LMS/CACE analysis of a single HT1080 cell in which virtually all of the substrate was in the phosphorylated form. (B) More representative LMS/CACE analysis of an HT1080 cell loaded as in A. (C) Analysis of an RBL cell loaded with F−PKB−C−SS−TAT (750 nM extracellular concentration). (D) Analysis of an RBL cell loaded with F−PKB−C−SS−TAT as in C and then incubated with PIP_3−histone.

(Figure 2B). Addition of DTT to the media surrounding these cells at the time of lysis converted the migration times of these peaks to that of nonphosphorylated F−PKB−C. These oxidized forms of F−PKB−C were either not accessible to PKB or not good substrates for PKB. In a minority of cells (15%, n = 15), only two peaks were present on the electrophoretic trace, and the migration times of these peaks were identical to that of nonphosphorylated and phosphorylated F−PKB−C. The percentage of peptide present as phosphorylated F−PKB−C in these cells was 75 ± 31%. This percentage of phosphorylated F−PKB−C was nearly identical to that measured when HT1080 cells were microinjected with F−PKB, suggesting that, in this subfraction of cells, all of the detected F−PKB−C was fully accessible to PKB (*30*). The amount of peptide detected with the LMS/CACE was quantitated by comparison to the standards, and on average, each cell possessed $7.0 \pm 1.2 \times 10^{-19}$ mol of detectable F−PKB−C. This represents a cytosolic concentration of ∼700 nM free F−PKB−C.

If an easily saturated step was present during the separation from TAT and reduction of the substrate, the inability of many HT1080 cells to maintain the F−PKB−C in its reduced form might have been due to the relatively high concentrations of F−PKB−C in the cell. For this reason, HT1080 cells were incubated in an extracellular concentration of 215 nM F−PKB−C−SS−TAT. At this lower concentration, 67% of the cells (n = 6) demonstrated electropherograms with only nonphosphorylated and phosphorylated F−PKB−C and no other peaks. The average amount of detected F−PKB−C in this subfraction of cells was $2.5 \pm 0.7 \times 10^{-19}$ mol. This

represents a cytosolic concentration of ~250 nM free F−PKB−C. To determine whether other cell types might also have a limited capacity to reduce the disulfide bond in F−PKB−C−SS−TAT, RBL cells were loaded with F−PKB−C−SS−TAT. All cells ($n = 3$) loaded at an extracellular concentration of 750 nM showed a peak with the same migration time as F−PKB−C and no additional peaks. These cells contained $1.4 \pm 0.2 \times 10^{-20}$ mol of detectable F−PKB−C, which represents an cytosolic concentration of ~14 nM. In contrast, when the extracellular concentration was increased to 3 μM, all RBL cells ($n = 4$) showed a multitude of peaks most of which did not possess migration times of nonphosphorylated or phosphorylated F−PKB−C. While achieving full reduction of F−PKB−C−SS−TAT was concentration-dependent, HT1080 and RBL cells loaded with F−CamKII−C−SS−TAT were rarely seen to demonstrate unexpected peaks regardless of the loading concentration used (<1 in 50 cells for an extracellular concentration range from 100 nM to 1 μM). Thus, F−CamKII−C appeared to be more easily maintained in the reduced state compared to F−PKB−C.

To determine whether the F−PKB−C delivered to cells by addition of F−PKB−C−SS−TAT (750 nM extracellular concentration) could also be phosphorylated after pharmacologic activation of PKB (rather than constitutively active PKB), PIP_3−histone was added to RBL cells. Exogenous phosphoinositides delivered to cells using cationic carriers, such as histone, have been demonstrated to activate PKB and exert downstream physiological responses (*39*, *44*). The LMS/CACE was used to analyze the amount of phosphorylated F−PKB−C in the presence (15 μM) and absence of PIP_3−histone added for 10 min to RBL cells loaded with F−PKB−C−SS−TAT (parts C and D of Figure 2). In RBL cells exposed to PIP_3−histone, 39 ± 14% ($n = 4$) of F−PKB−C was phosphorylated, while no phosphorylation was present in unexposed cells.

Design of a Substrate Peptide Linked to TAT(49−57) by a Photolabile Bond. While substrate peptides disulfide-linked to TAT(49−57) could in some instances be delivered to the cytosol in a fully reduced form accessible to the intended kinases, this was not always the case. Therefore, we designed a second detachable linker between the TAT(49−57) and the substrate peptide. An Fmoc-aminoethyl photolabile moiety was inserted between the fluorescently labeled substrate and the TAT(49−57) sequences using standard Fmoc peptide chemistry. The relative order of the different portions of the conjugate was fluorescein−substrate−PLL−TAT(49−57). Two different substrate peptides were conjugated to the TAT(49−57) to form F−PKB−PLL−TAT and F−CamKII−PLL−TAT. To determine the time and irradiation intensity needed to photocleave the conjugated peptides, standard solutions (1 nM or 10 μM) of F−PKB−PLL−TAT were illuminated with long-wavelength UV light (UVA) for varying times. The sample was then loaded into a capillary and electrophoresed. The concentration of the released substrate peptide was quantitated from its fluorescence. At the irradiation intensity and peptide concentrations used, maximal cleavage of the substrate peptide from the TAT sequence was achieved within 20 min (Figure 3). After an exposure for 10 s, 2% of the conjugate was photoreleased. Without UVA illumination, no free substrate peptide could be detected in electrophoretic separations. The fluorescein

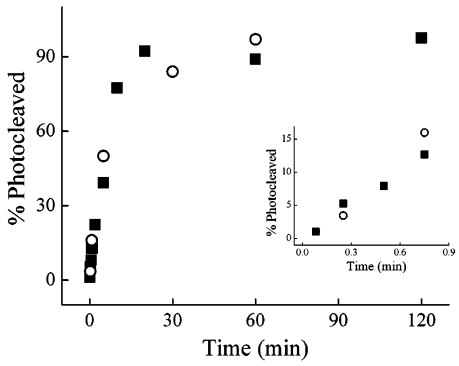

FIGURE 3: Time course of cleavage of the F−PKB−PLL−TAT. (A) In vitro production of free F−PKB after UVA irradiation of a solution of F−PKB−PLL−TAT (1 nM, ■; 10 μM, ○) for varying times. (B) Expanded view of the graph for times ≤1 min.

was not substantially photobleached by the UVA-induced cleavage because the amount of fluorescent peptide detected after an irradiation for 4 h was almost identical to that after 20 min of UVA exposure.

Characterization of Photocleavable Substrate−TAT(49−57) Conjugates in Cells. HT1080/PTEN cells were loaded with F−PKB−PLL−TAT (1 μM extracellular concentration) in a manner identical to the loading of the disulfide conjugates. After loading, the cells were illuminated with UVA light for 10 s, washed, and then incubated an additional 10 min. Single cells were then selected for LMS/CACE analysis. In contrast to the disulfide conjugate, nearly all electrophoretic traces ($n = 6$) possessed a single peak with a migration time identical to that of a standard of F−PKB (Figure 4A). While the F−PKB−PLL−TAT was taken into the cell and a portion of the F−PKB was successfully detached from the TAT(49−57) sequence, it was unlikely that all of the F−PKB was photoreleased because of the very short irradiation time. The measured F−PKB represents only the photocleaved portion of the conjugate because the intact F−PKB−PLL−TAT could not be detected because of its adsorption onto the capillary walls as discussed above. As expected, phosphorylation of the released F−PKB was not seen in HT1080/PTEN cells.

To determine whether a substrate peptide other than F−PKB could also be successfully loaded into cells as a photolabile conjugate, HT1080 cells were incubated with F−CamKII−PLL−TAT (100 nM). When this conjugate was photocleaved in the cells, a single peak with a migration time identical to that of the F−CamKII standard was present on nearly all electropherograms ($n > 10$) (Figure 4C).

Exposure to ultraviolet wavelengths of light can activate stress-related pathways in cells particularly those involving the phosphorylation and activation of PKB and the p38 MAP kinase (*45*−*48*). Because HT1080 cells already have activated PKB and p38 MAP kinase, this cell line could not be used to determine whether the exposure for 10 s to UVA light activated these kinases. The HT1080/PTEN cells overexpress PTEN and therefore might be more resistant to UVA-induced activation of PKB. For these reasons, serum-starved 3T3 cells were exposed to UVA light in a manner identical to that used for photocleavage of the reporters in cells. The cells were then analyzed by Western blot for phosphorylated PKB and p38 MAP kinase. Cells illuminated with UVA light for 10 and 30 s possessed equivalent amounts

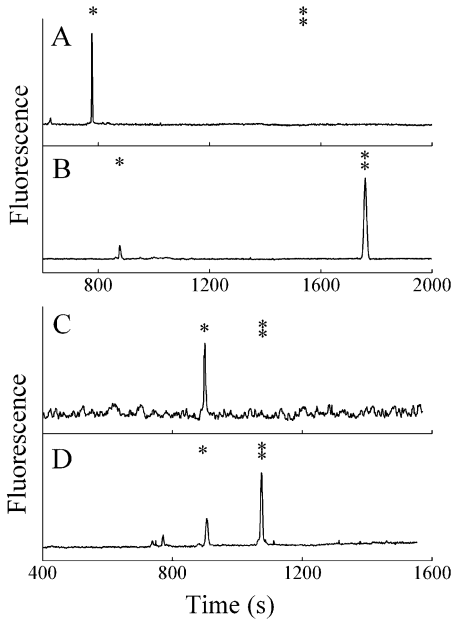

FIGURE 4: Analysis of single cells loaded with peptide substrates conjugated to TAT(49−57) through a photolabile bond. Representative electrophoretic traces from the LMS/CACE analyses of cells loaded with F−PKB−PLL−TAT or F−CamKII−PLL−TAT. A single asterisk denotes the migration time of F−PKB or F−CamKII, and a double asterisk denotes the migration time of phosphorylated F−PKB or phosphorylated F−CamKII from cells on the day of the experiment. (A) Electrophoretic trace from the LMS/CACE analysis of a single HT1080/PTEN cell loaded with F−PKB−PLL−TAT (1 μM). (B) Electrophoretic trace from the LMS/CACE analysis of a single HT1080 cell loaded with F−PKB−PLL−TAT (1 μM). The cells in A and B were investigated with different capillaries, accounting for the variation in migration times. (C) Analysis of an HT1080 cell loaded with F−CamKII−PLL−TAT (300 nM). (D) Analysis of an HT1080 loaded with F−CamKII−PLL−TAT (300 nM) and then incubated with ionomycin (500 nM) for 5 min. The experiments in C and D were performed utilizing the same capillary.

of phosphorylated PKB or phosphorylated p38 MAP kinase compared to cells not exposed to UVA (data not shown). The duration and intensity of UVA illumination used for photocleavage was not sufficient to activate these kinases.

Phosphorylation of Substrate Peptides Delivered by a Photocleavable TAT(49−57). HT1080 cells were loaded with F−PKB−PLL−TAT (1 μM extracellular concentration) in an identical manner to that of the HT1080/PTEN cells above. When the contents of the HT1080 cells were analyzed with the LMS/CACE, nearly all electrophoretic traces possessed only two peaks with the migration times similar to that of F−PKB or phosphorylated F−PKB (Figure 4B). A total of 67 ± 27% (n = 15) of the F−PKB was present in the phosphorylated form. These results were nearly identical to those measured when F−PKB was microinjected or loaded successfully with the disulfide conjugate (*30*). These data suggest that all detected F−PKB is accessible to PKB, i.e., in the cytosol.

To determine whether a substrate peptide for CamKII could be phosphorylated when loaded into cells as a photolabile conjugate, HT1080 cells were incubated with F−CamKII−PLL−TAT (300 nM). Ionomycin (500 nM) was then added to the cells, and the cells were incubated for 15 min. Two major peaks were present on the electrophoretic trace of the contents of the cell (Figure 4D). The migration times of the peaks were similar to that of the nonphosphorylated and phosphorylated standards of F−CamKII loaded into the cells. On average, 67 ± 17% (n = 3) of the total F−CamKII was phosphorylated.

To determine the total amount of free F−PKB released into the cytoplasm and detectable by the LMS/CACE, HT1080 cells were incubated with F−PKB−PLL−TAT (1 μM) for 5 min and then washed. After an incubation for 30 min, cells were UVA-irradiated for 10 s, allowed to recover for 10 min, and analyzed with the LMS/CACE. The average quantity of F−PKB detected per cell was $2.0 \pm 0.9 \times 10^{-19}$ mol (n = 15). This value represents an approximate cytoplasmic concentration of 200 nM of free F−PKB. When HT1080 cells were loaded with F−CamKII−PLL−TAT (300 nM extracellular concentration), each cell possessed $1.8 \pm 1.9 \times 10^{-19}$ mol (n = 3) of detectable F−CamKII. This represents an average concentration of ~180 nM F−CamKII in the cytosol of the cells.

Time Dependence of Cytosolic Entry and Accessibility of TAT-Loaded Cargo. Prior work suggests that the initial step in TAT-mediated import of cargo into a cell is the adsorption of TAT to the surface of the cell presumably via an electrostatic interaction (*8*, *49*). The next step involving internalization of the TAT−cargo into the cell appears to be a much slower process and may be mediated by endocytosis or another mechanism. Recent work by Fittapaldi et al. demonstrated that for intact, folded proteins this second step required as long as 10 h to reach completion (*22*). This result contrasts with other studies that measured very fast uptake times for TAT and its cargo (*13*, *24*, *50*). One possible explanation is that the different methods used might detect TAT at different steps during its uptake into a cell. For this reason, we measured the time required for TAT-mediated delivery of F−PKB into the cytosol and the time required for F−PKB to become accessible to PKB after adsorption of TAT−PLL−PKB onto the plasma membrane. HT1080 cells were incubated with F−PKB−PLL−TAT (1 μM extracellular concentration) at 37 °C for 5 min to adsorb TAT onto the cell surface. The cells were washed removing all F−PKB−PLL−TAT dissolved in the media and were then incubated for varying times at 37 °C. After this incubation time, the cells were irradiated for 10 s with UVA light and analyzed with the LMS/CACE. The total amount of F−PKB detected with the LMS/CACE increased over the initial hour of incubation and then stabilized (Figure 5A). This result suggests that, for short peptide cargoes, the internalization process into the cytosol is complete within 1 h. The percentage of phosphorylated F−PKB was similar to that measured previously in HT1080 cells and did not vary with the incubation time (Figure 5A). These data suggest that all F−PKB detected by LMS/CACE is accessible to cytosolic kinases. Compartmentalized F−PKB not accessible to cytosolic kinase does not appear to be detected by LMS/CACE.

Temperature Dependence of Cytosolic Entry and Accessibility of TAT-Loaded Cargo. Previous experiments measuring the temperature dependence of TAT-mediated translocation has yielded discrepant results. Some of these differences may be due to TAT adsorption to the surface of the cell, which occurs at all temperatures, whereas actual internalization may be much more heavily dependent on temperature (*14*). Adsorbed TAT that was loaded into the cell after removal of the soluble TAT might then be indistinguishable from that loaded into the cell during the time the cell was

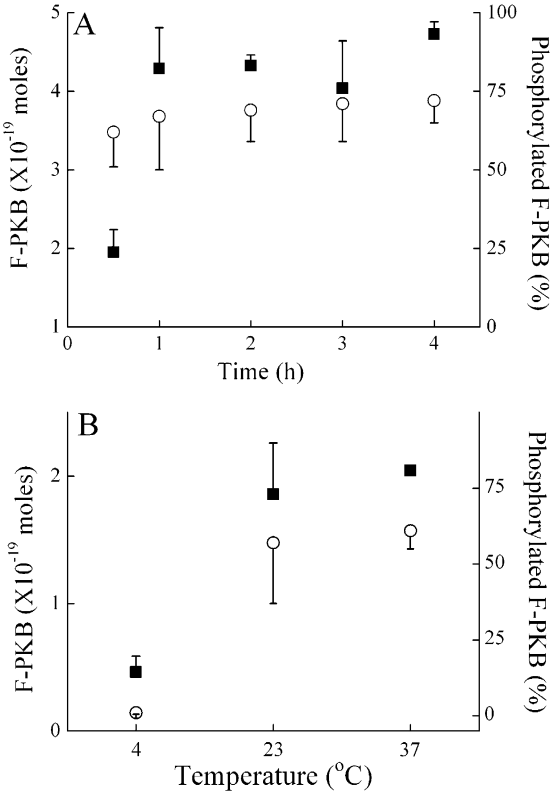

FIGURE 5: Time and temperature dependence of cytosolic entry and accessibility of TAT-loaded cargo. (A) Time dependence of the amount of detectable F−PKB (left axis, ■) and the percentage phosphorylation of that F−PKB (right axis, ○) per HT1080 cell (n = 4 for each point). (B) Temperature dependence of the amount of detectable F−PKB (left axis, ■) and the percentage phosphorylation of that F−PKB (right axis, ○) per HT1080 cell (n = 4 for each point). Each point reflects the average measurement value, and the error bars represent the standard error. The error bars are shown in only one direction for clarity.

incubated with soluble TAT. HT1080 cells were loaded with F−PKB−PLL−TAT (1 μM extracellular concentration) as described in the Experimental Procedures, except that the loading and incubation steps were performed at either 4, 23, or 37 °C. The cells were then immediately analyzed with the LMS/CACE while still in the solution at 4, 23, or 37 °C. The amount of F−PKB measured per cell was similar at both 23 and 37 °C but was reduced in cells maintained at 4 °C (Figure 5B). Loading does occur at low temperature, although with less efficiency than at higher temperatures. Because the percentage of phosphorylated F−PKB was similar at 23 and 37 °C, the cargo was readily available for phosphorylation when released from TAT at these temperatures. At 4 °C, essentially no phosphorylation occurred (Figure 5B). This was most likely due to decreased kinase activity rather than to inaccessible F−PKB, although the two possibilities cannot be distinguished from these experiments.

Determination of the Percentage of F−PKB−PLL−TAT Photocleaved in Cells. To estimate the percentage of F−PKB−PLL−TAT that was cleaved by 10 s of UVA light, RBL cells were loaded with F−PKB−PLL−TAT for 10 min and washed as described in the Experimental Procedures. The cells were then placed in DMEM supplemented with 10% FCS for 1 h at 37 °C. After 1 h, the internalization process is complete and all F−PKB−PLL−TAT that can enter the cytosol has done so (Figure 5A). Thus, the total concentration of all forms of F−PKB (F−PKB, phosphorylated F−PKB, and F−PKB−PLL−TAT) in the cytosol of a cell should be nearly constant in all subsequent experimental steps. The cells were then placed on ice for 30 min. During this time, the cells were illuminated with UVA light for either 10 s or 30 min. The ice prevented the cell solution from heating during the longer UVA exposure time. The illumination time of 30 min was performed to photocleave all F−PKB−PLL−TAT within the cytosol (see Figure 3), so that the total amount of F−PKB−PLL−TAT loaded into the cytosol could be measured. After incubation on ice, cells were immediately analyzed with the LMS/CACE and the total amount of F−PKB (phosphorylated plus nonphosphorylated) was quantitated by comparison to the standards. After 10 s of UVA illumination, $12 \pm 7 \times 10^{-20}$ mol (n = 3) of total F−PKB was detected on the electrophoretic traces. After photocleavage for 30 min, $18 \pm 4 \times 10^{-19}$ mol (n = 3) was detectable. Cells not exposed to UVA light did not possess free substrate peptide. Therefore, ∼7% of the cytosolic F−PKB−PLL−TAT was photocleaved after 10 s of UVA illumination. This result is similar to that photoreleased (∼2%) following an illumination of 10 s for a cell-free solution of F−PKB−PLL−TAT.

Determination of the Total Amount of F−PKB−PLL−TAT Loaded into Cells. To determine the total amount of F−PKB−PLL−TAT (cytosolic plus compartmentalized) loaded into cells, HT1080 cells were loaded with F−PKB−PLL−TAT and lysed and their contents were electrophoresed in the standard electrophoretic buffer with or without Triton X-100 (10%). High concentrations of Triton X-100 are very effective at solubilizing cellular membranes and thus releasing the contents of membrane-bound organelles (*51*). The cells were initially loaded with F−PKB−PLL−TAT for 10 min and washed as described in the methods. The cells were then placed in DMEM supplemented with 10% FCS for 1 h at 37 °C. To photocleave all cellular F−PKB−PLL−TAT, the cells were illuminated with UVA light for 30 min (while on ice). Again the photocleavage time of 30 min was utilized so that all F−PKB−PLL−TAT would be converted into a detectable form (F−PKB or phosphorylated F−PKB). Single cells were then analyzed with the LMS/CACE. In the first experiment, the standard electrophoretic buffer was used and the average amount of total F−PKB (phosphorylated plus nonphosphorylated) was $16 \pm 4 \times 10^{-19}$ mol per cell (n = 4). In a second experiment, single cells were lysed and loaded electrophoretically into an LMS/CACE capillary containing the standard electrophoretic buffer plus Triton X-100 (10%). The capillary was then manually translated into a vial containing the electrophoretic buffer plus Triton X-100 (10%), and electrophoresis reinitiated. The average amount of F−PKB detected in these cells was $19 \pm 6 \times 10^{-19}$ mol (n = 3). Under these conditions, the majority of the F−PKB in the cell has exited subcellular compartments accessible with 10% Triton X-100. Because Triton X-100 will lyse all membrane-bound compartments including endosomes, these data suggest that nearly all F−PKB has exited cellular subcompartments within 1 h. However, when incubation times substantially shorter than 1 h are employed, some F−PKB (free or conjugated to TAT) will likely remain in subcellular compartments.

Physiologic Phosphorylation of F−PKB Delivered into 3T3 Cells By F−PKB−PLL−TAT. If F−PKB delivered by F−PKB−PLL−TAT is fully accessible to cellular PKB, then

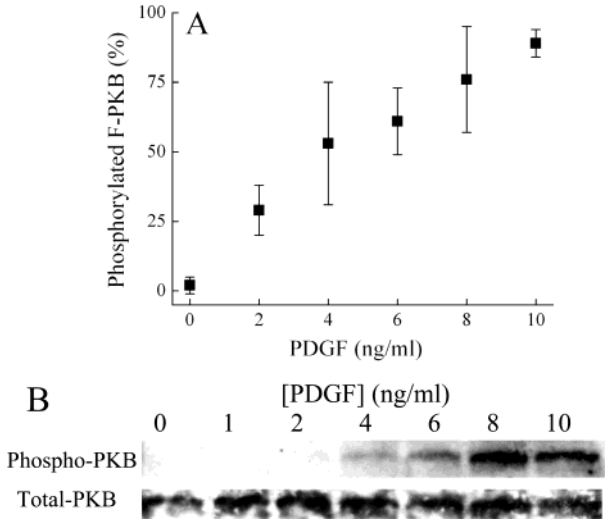

FIGURE 6: Measurement of the activation of PKB following a physiologic stimulus. 3T3 cells were incubated with varying concentrations of PDGF for 10 min at 37 °C. (A) Cells were previously loaded with F−PKB using F−PKB−PLL−TAT, and the percentage of phosphorylated F−PKB was measured in single cells after application of PDGF. The average measurement of a minimum of 5 cells for each PDGF concentration with the error bars representing the standard deviation is shown. (B) Cells were incubated with PDGF and then lysed. Western blots using antibodies against phospho-PKB (see the Experimental Procedures) were then performed on the lysates. Antibodies against PKB were used to assess the total amount of PKB per lane.

the percentage of phosphorylated F−PKB should yield a quantitative measure of cellular PKB activation following application of a physiologic stimuli. To test this hypothesis, PDGF at varying concentrations was added to serum-starved 3T3 cells preloaded with F−PKB utilizing F−PKB−PLL−TAT (as described in the Experimental Section). After 10 min, single cells were analyzed by LMS/CACE to determine the ratio of phosphorylated F−PKB to total F−PKB (Figure 6A). A second set of 3T3 cells were stimulated with PDGF in an identical manner and then analyzed by Western blot for phosphorylated PKB (as an indirect measure of the activation of PKB in cells) (Figure 6B). The average amount of phosphorylated F−PKB measured by LMS/CACE paralleled the phosphorylation of PKB as measured by Western blot. At a low PDGF concentration (2 ng/mL) phosphorylation of F−PKB was easily detected by LMS/CACE, while the Western blot possessed an extremely faint band (difficult to visualize in the reproduced figure). Thus, LMS/CACE measurement of phosphorylated F−PKB yielded a more sensitive and quantitative measure of PKB activity compared to Western blot analysis of phosphorylated PKB.

DISCUSSION

A goal of this paper was to determine whether cargo delivered by TAT(49−57) was present in the cytosol and in a form accessible to cytosolic proteins. The PKB substrate successfully loaded into cells using the photolabile or disulfide conjugates was phosphorylated to the same degree at steady state as the microinjected substrate, demonstrating its accessibility to cytosolic kinases (*30*). At least a portion (and potentially all) of the CamKII substrate transported into the cytosol by the TAT sequence was also accessible because over 50% was phosphorylated after CamKII activation. When photolabile conjugates were used, both free and conjugated substrate were present in the cytosol because the UVA light exposure was sufficient to cleave only a fraction of the conjugated peptide. The presence of cytosolic F−PKB−PLL−TAT substrate did not interfere with phosphorylation/dephosphorylation of free F−PKB. The most likely explanation is that the TAT conjugates were very poor substrates and so did not interfere with free substrate phosphorylation.

Other investigators have demonstrated that the vast majority (>90%) of TAT-linked cargo may reside in endosomes rather than in the cytosol (*14*, *22*). In contrast, our results suggest that small peptide cargoes delivered to cells at low concentrations are not trapped permanently within subcellular compartments. A total of 1 h after administration to the cells, nearly all of the cargo is present in the cytosol and accessible to cytosolic kinases. At times, less than an hour after exposure to the TAT conjugate, not all cargo (or substrate peptide) is present in the cytosol. However, the LMS/CACE does not appear to sample significant amounts of compartmentalized, free substrate because the steady-state level of phosphorylated PKB substrate in HT1080 cells was nearly identical to that seen in cells microinjected with free F−PKB. Selective sampling of the cytosolic compartment is most likely an attribute of the laser-based sampling method because the extent of lysis of cellular subcompartments has been demonstrated to depend on the amount of energy deposited by the laser pulse. Low−intermediate energies similar to those employed in these experiments disrupt the plasma membrane but leave many organelles intact (*29*, *34*). Peptide sequestered in organelles such as endosomes would therefore be loaded into the capillary inside the intact compartment. This compartmentalized peptide would not comigrate with the free peptide in the cytosol, because the migration of the organelles through the capillary would be substantially different from that of the free substrate because of the large differences in their mass, shape, and charge. Under the electrophoretic conditions used, this peptide would most likely never reach the detection zone and is consequently not detected by LMS/CACE under these conditions. However, use of the LMS/CACE method with other electrophoretic conditions or at higher laser-pulse energies might permit sampling of a broader array of cellular compartments (*34*, *52*).

When TAT was conjugated to F−PKB−C by a disulfide bond and incubated with cells at high concentrations (≥ ∼1 μM), a variety of different forms of F−PKB−C were present in the cells. These forms could all be reduced to F−PKB−C upon addition of DTT. This attribute was not peculiar to HT1080 cells because RBL cells also exhibited similar peaks that were reducible to F−PKB−C with DTT. In contrast, the F−CamKII−C detected from these cells was always fully reduced. Cells typically possess 1−10 mM cytosolic glutathione, with ∼99% in the reduced form (GSH) and ∼1% in a disulfide-bound form (GS−SG) (*53*). Rapidly dividing cells such as tumor cells often possess much higher levels of glutathione than normal cells (*54*). Consequently, it is unlikely that the HT1080 or RBL cells were deficient in their glutathione content or in their ability to reduce disulfide bonds relative to other cells. Hallbrink et al. measured the in vitro rate of separation of membrane-permeant sequences linked to a cargo by a disulfide bond after addition of GSH (*24*). The TAT sequence possessed a 4−10-fold higher rate constant for separation than other tested membrane-permeant sequences. They concluded that reduction of disulfide-linked

TAT and cargo would occur extremely rapidly compared to the rate at which TAT−cargo enters the cell. These data suggest that the F−PKB−C is rapidly separated from the TAT upon entry into the cytosol but that the Cys on this substrate remains in an oxidized state. It is possible that the F−PKB−C is more prone to reactions involving the sulfur compared to the F−CamKII−C. This may be due to the properties of the PKB substrate sequence near the disulfide bond. A final potential explanation for the TAT-released, oxidized forms of F−PKB−C is that they are produced in an oxidizing compartment, i.e., endosomes. These oxidized species may then cross into the cytoplasmic compartment where the reducing potential may not be suitable to reduce these oxidation products.

Photolabile TAT conjugates displayed a number of advantages in peptide delivery compared to the disulfide-linked forms. The photolabile conjugate did not require the addition of a cysteine to the substrate peptide, thus eliminating the undesirable reactions of the sulfur and preventing potential changes in the kinetic properties of the kinase substrate because of the addition of the cysteine (*55*). With the photolabile bond, it was also possible to control the timing and extent of substrate release from the TAT. One potential weakness of the photolabile construct is that exposure of cells to UVA light has been shown to induce activation of a number of kinases including phosphatidylinositol 3-kinase (PI3K), which is upstream of PKB, and the mitogen-activated protein kinases, particularly p38 MAP kinase (*45*−*48*). We did not detect the phosphorylation and therefore activation of these kinases in cells exposed to the UVA light for times triple that used to photocleave the reporters. In addition, the total light power per unit area required to activate PKB in published experiments was considerably higher than that utilized in these experiments. For example, Zhang and co-workers have shown that PI3K and PKB were activated in cultured mouse epidermal cells by exposure to UVA at 160 kJ/m^2 (*48*). Others have shown that UVA exposure at 800 J/m^2 was not sufficient to activate the PI3K pathway (*47*). On the basis of this prior work and our current experimental work, the dose of UVA (1 kJ/m^2) used did not activate stress-related pathways. This conclusion is also supported by the lack of phosphorylation of F−PKB in the HT1080/PTEN cells loaded with F−PKB−PLL−TAT. In these cells, the inhibition because of PTEN overexpression is reversible by application of additional stimuli activating the PI3K pathway, for example, serum or PDGF (*42*).

Many reports have indicated that the primary driving force behind TAT-mediated transduction is endocytosis, while others have provided support for nonendocytic mechanisms (*14*, *19*, *22*, *56*). Evidence suggests that some of these discrepancies may be due to artifacts created by the cell fixation procedures or by the high avidity of the TAT sequence for the plasma membrane (*14*, *57*). The approach used in this study did not require fixation of the cells. In addition, only cargo released from the TAT carrier was sampled, preventing artifacts from conjugated peptide adsorbed to the cell surface or conjugated peptide not yet delivered to the cytosol. In some recent studies, the potential for artifacts because of cell fixation and nonspecific adsorption have been investigated (*14*, *22*, *58*). These studies show impairment but not an absence of loading at low temperatures (∼4−23 °C) compared to 37 °C. Our results agree with these data showing a 4-fold increase in the amount of substrate peptide per cell from 4 to 37 °C. These data suggest that an energy-independent mechanism may still contribute to TAT-mediated internalization (or that the energy-dependent components are not completely inhibited at low temperatures). After an exposure for 5 min to the TAT conjugate at 37 °C, the amount of peptide subsequently internalized and released into the cytosol increased over the first hour and then stabilized. This finding is consistent with prior work studying the cargo delivery kinetics of a TAT-conjugated peptide, although in that study the cell was continuously exposed to the conjugate so the effects of adsorption to the surface were not taken into account (*24*). However, these data are in contrast to a recent report showing a time course of 10 h for the uptake of TAT conjugated to the enhanced GFP (*22*). These rate disparities may be due to the different cell types used or to the structural stability and size of the different cargoes attached to the TAT sequence (peptide versus folded protein). The GFPs, approximately 30 kD in mass, have a highly stable, β-barrel structure in contrast to the roughly 1.5 kD substrate peptides, which adopt a random conformation.

The ratio of the cytosolic concentration of free substrate to the extracellular concentration of the TAT-conjugated substrate was between ∼1:20 and ∼1:1. This contrasts with most prior experimental data suggesting ratios of >100:1 or much higher intracellular/extracellular TAT−cargo concentrations (*14*, *22*). However, compared to other methods of loading membrane-impermeant molecules into cells, the cleavable TAT conjugates were very effective. Microinjection, optoporation, and pinocytic loading typically yield a 1:100 ratio of free cytosolic/extracellular (or injection pipet) concentration (unpublished data and refs *27*, *59*). With the cleavable TAT conjugates, nanomolar−micromolar concentrations of the substrate peptides were rapidly and easily loaded into the cytosol.

A second attribute of the cleavable TAT conjugates was the lack of activation of stress-induced, membrane-repair, or proteolytic pathways, which can be stimulated following pinocytic loading or microinjection. CamKII, which is activated by increases in the intracellular free Ca^{2+} concentration and by membrane-repair pathways, did not phosphorylate F−CamKII except in the presence of ionomycin (*60*, *61*). PKB, a kinase frequently activated under conditions of cellular stress, did not phosphorylate F−PKB in the cell types lacking constitutively active PKB. Both CamKII and PKB can be activated with some of the other loading methods (unpublished data and refs *27*, *59*). Unidentified peaks (not reducible with DTT) are usually indicative of proteolytic breakdown of the substrate peptide (unpublished data and refs *27*, *59*). These "proteolytic" peaks frequently occur when a poor microinjection technique is employed but were not present on the electrophoretic traces of cells loaded with TAT conjugates. With these concentrations and conditions, the TAT conjugates efficiently loaded kinase substrates into the cytosol without activating stress-induced pathways or increasing proteolytic activity in the cells.

ACKNOWLEDGMENT

The authors thank G. Meredith, A. Hong, and J. Audet for helpful discussions. N.L.A., C.E.S., and F.M.R. disclose financial interests in Cell Biosciences, Inc.

REFERENCES

1. Lipinski, C. A., Lombardo, F., Dominy, B. W., and Feeney, P. J. (2001) Experimental and computational approaches to estimate solubility and permeability in drug discovery and development settings, *Adv. Drug Deliv. Rev. 46*, 3−26.
2. Ribeiro, M. M., Klein, D., Pileggi, A., Molano, R. D., Fraker, C., Ricordi, C., Inverardi, L., and Pastori, R. L. (2003) Heme oxygenase-1 fused to a TAT peptide transduces and protects pancreatic β-cells, *Biochem. Biophys. Res. Commun. 305*, 876−881.
3. Stein, S., Weiss, A., Adermann, K., Lazarovici, P., Hochman, J., and Wellhoner, H. (1999) A disulfide conjugate between anti-tetanus antibodies and HIV (37−72)TAT neutralizes tetanus toxin inside chromaffin cells, *FEBS Lett. 458*, 383−386.
4. Stolzenberger, S., Haake, M., and Duschl, A. (2001) Specific inhibition of interleukin-4-dependent Stat6 activation by an intracellularly delivered peptide, *Eur. J. Biochem. 268*, 4809−4814.
5. Shibagaki, N., and Udey, M. C. (2003) Dendritic cells transduced with TAT protein transduction domain-containing tyrosinase-related protein 2 vaccinate against murine melanoma, *Eur. J. Immunol. 33*, 850−860.
6. Cao, G., Pei, W., Ge, H., Liang, Q., Luo, Y., Sharp, F. R., Lu, A., Ran, R., Graham, S. H., and Chen, J. (2002) In Vivo Delivery of a Bcl-xL Fusion Protein Containing the TAT Protein Transduction Domain Protects against Ischemic Brain Injury and Neuronal Apoptosis, *J. Neurosci. 22*, 5423−5431.
7. Becker-Hapak, M., McAllister, S. S., and Dowdy, S. F. (2001) TAT-mediated protein transduction into mammalian cells, *Methods 24*, 247−256.
8. Wadia, J. S., and Dowdy, S. F. (2002) Protein transduction technology, *Curr. Opin. Biotechnol. 13*, 52−56.
9. Lindsay, M. A. (2002) Peptide-mediated cell delivery: Application in protein target validation, *Curr. Opin. Pharmacol. 2*, 587−594.
10. Green, M., and Loewenstein, P. M. (1988) Autonomous functional domains of chemically synthesized human immunodeficiency virus TAT trans-activator protein, *Cell 55*, 1179−1188.
11. Frankel, A. D., and Pabo, C. O. (1988) Cellular uptake of the TAT protein from human immunodeficiency virus, *Cell 55*, 1189−1193.
12. Vogel, B. E., Lee, S. J., Hildebrand, A., Craig, W., Pierschbacher, M. D., Wong-Staal, F., and Ruoslahti, E. (1993) A novel integrin specificity exemplified by binding of the α vs β 5 integrin to the basic domain of the HIV TAT protein and vitronectin, *J. Cell Biol. 121*, 461−468.
13. Wender, P. A., Mitchell, D. J., Pattabiraman, K., Pelkey, E. T., Steinman, L., and Rothbard, J. B. (2000) The design, synthesis, and evaluation of molecules that enable or enhance cellular uptake: Peptoid molecular transporters, *Proc. Natl. Acad. Sci. U.S.A. 97*, 13003−13008.
14. Richard, J. P., Melikov, K., Vives, E., Ramos, C., Verbeure, B., Gait, M. J., Chernomordik, L. V., and Lebleu, B. (2003) Cell-penetrating peptides. A reevaluation of the mechanism of cellular uptake, *J. Biol. Chem. 278*, 585−590.
15. Schwarze, S. R., Ho, A., Vocero-Akbani, A., and Dowdy, S. F. (1999) In vivo protein transduction: Delivery of a biologically active protein into the mouse, *Science 285*, 1569−1572.
16. Lewin, M., Carlesso, N., Tung, C. H., Tang, X. W., Cory, D., Scadden, D. T., and Weissleder, R. (2000) TAT peptide-derivatized magnetic nanoparticles allow in vivo tracking and recovery of progenitor cells, *Nat. Biotechnol. 18*, 410−414.
17. Green, I., Christison, R., Voyce, C. J., Bundell, K. R., and Lindsay, M. A. (2003) Protein transduction domains: Are they delivering? *Trends Pharmacol. Sci. 24*, 213−215.
18. Derossi, D., Calvet, S., Trembleau, A., Brunissen, A., Chassaing, G., and Prochiantz, A. (1996) Cell internalization of the third helix of the Antennapedia homeodomain is receptor-independent, *J. Biol. Chem. 271*, 18188−18193.
19. Vives, E., Brodin, P., and Lebleu, B. (1997) A truncated HIV-1 TAT protein basic domain rapidly translocates through the plasma membrane and accumulates in the cell nucleus, *J. Biol. Chem. 272*, 16010−16017.
20. Futaki, S., Suzuki, T., Ohashi, W., Yagami, T., Tanaka, S., Ueda, K., and Sugiura, Y. (2001) Arginine-rich peptides. An abundant source of membrane-permeable peptides having potential as carriers for intracellular protein delivery, *J. Biol. Chem. 276*, 5836−5840.
21. Suzuki, T., Futaki, S., Niwa, M., Tanaka, S., Ueda, K., and Sugiura, Y. (2002) Possible existence of common internalization mechanisms among arginine-rich peptides, *J. Biol. Chem. 277*, 2437−2443.
22. Fittipaldi, A., Ferrari, A., Zoppe, M., Arcangeli, C., Pellegrini, V., Beltram, F., and Giacca, M. (2003) Cell membrane lipid rafts mediate caveolar endocytosis of HIV-1 TAT fusion proteins, *J. Biol. Chem. 278*, 34141−34149.
23. Potocky, T. B., Menon, A. K., and Gellman, S. H. (2003) Cytoplasmic and nuclear delivery of a TAT-derived peptide and a β-peptide after endocytic uptake into HeLa cells, *J. Biol. Chem. 278*, 50188−50194.
24. Hallbrink, M., Floren, A., Elmquist, A., Pooga, M., Bartfai, T., and Langel, U. (2001) Cargo delivery kinetics of cell-penetrating peptides, *Biochim. Biophys. Acta 1515*, 101−109.
25. Kelemen, B. R., Hsiao, K., and Goueli, S. A. (2002) Selective in vivo inhibition of mitogen-activated protein kinase activation using cell-permeable peptides, *J. Biol. Chem. 277*, 8741−8748.
26. Astriab-Fisher, A., Sergueev, D., Fisher, M., Shaw, B. R., and Juliano, R. L. (2002) Antisense inhibition of P-glycoprotein expression using peptide−oligonucleotide conjugates, *Pharm. Res. 19*, 744−754.
27. Meredith, G. D., Sims, C. E., Soughayer, J. S., and Allbritton, N. L. (2000) Measurement of kinase activation in single mammalian cells, *Nat. Biotechnol. 18*, 309−312.
28. Li, H., Wu, H. Y., Wang, Y., Sims, C. E., and Allbritton, N. L. (2001) Improved capillary electrophoresis conditions for the separation of kinase substrates by the laser micropipet system, *J. Chromatogr., B 757*, 79−88.
29. Sims, C. E., Meredith, G. D., Krasieva, T. B., Berns, M. W., Tromberg, B. J., and Allbritton, N. L. (1998) Laser-micropipet combination for single-cell analysis, *Anal. Chem. 70*, 4570−4577.
30. Li, H., Sims, C. E., Kaluzova, M., Stanbridge, E. J., and Allbritton, N. L. (2004) A quantitative single-cell assay for protein kinase B reveals important insights into the biochemical behavior of an intracellular substrate peptide, *Biochemistry* 43, 1599−1608.
31. Hanson, P. I., Kapiloff, M. S., Lou, L. L., Rosenfeld, M. G., and Schulman, H. (1989) Expression of a multifunctional Ca2+/calmodulin-dependent protein kinase and mutational analysis of its autoregulation, *Neuron 3*, 59−70.
32. Alessi, D. R., Caudwell, F. B., Andjelkovic, M., Hemmings, B. A., and Cohen, P. (1996) Molecular basis for the substrate specificity of protein kinase B; Comparison with MAPKAP kinase-1 and p70 S6 kinase, *FEBS Lett. 399*, 333−338.
33. Pain, D., and Surolia, A. (1981) Preparation of protein A-peroxidase monoconjugate using a heterobifunctional reagent, and its use in enzyme immunoassays, *J. Immunol. Methods 40*, 219−230.
34. Li, H., Sims, C. E., Wu, H. Y., and Allbritton, N. L. (2001) Spatial control of cellular measurements with the laser micropipet, *Anal. Chem. 73*, 4625−4631.
35. Wang, Y., Hu, S., Li, H., Allbritton, N. L., and Sims, C. E. (2003) Separation of mixtures of acidic and basic peptides at neutral pH, *J. Chromatogr., A 1004*, 61−70.
36. Weinberger, R. (2000) *Practical Capillary Electrophoresis*, Academic Press, San Diego, CA.
37. Fishman, H. A., Scheller, R. H., and Zare, R. N. (1994) Microcolumn sample injection by spontaneous fluid displacement, *J. Chromatogr., A 680*, 99−107.
38. Crank, J. (1989) *The Mathematics of Diffusion*, Clarendon Press, Oxford, U.K.
39. Weiner, O. D., Neilsen, P. O., Prestwich, G. D., Kirschner, M. W., Cantley, L. C., and Bourne, H. R. (2002) A PtdInsP(3)- and Rho GTPase-mediated positive feedback loop regulates neutrophil polarity, *Nat. Cell Biol. 4*, 503−513.
40. Meister, A. (1989) in *Glutathione: Chemical, Biochemical, and Medical Aspects* (Dolphin, D., Poulson, R., and Avramovic, O., Eds.) pp 367−474, Wiley, New York.
41. Gupta, S., Plattner, R., Der, C. J., and Stanbridge, E. J. (2000) Dissection of Ras-dependent signaling pathways controlling aggressive tumor growth of human fibrosarcoma cells: Evidence for a potential novel pathway, *Mol. Cell. Biol. 20*, 9294−9306.
42. Gupta, S., and Stanbridge, E. J. (2001) Paired human fibrosarcoma cell lines that possess or lack endogenous mutant N-ras alleles as experimental model for Ras signaling pathways, *Methods Enzymol. 333*, 290−306.

43. Worrell, R. T., and Frizzell, R. A. (1991) CaMKII mediates stimulation of chloride conductance by calcium in T84 cells, *Am. J. Physiol. 260*, C877−C882.
44. Wang, F., Herzmark, P., Weiner, O. D., Srinivasan, S., Servant, G., and Bourne, H. R. (2002) Lipid products of PI(3)Ks maintain persistent cell polarity and directed motility in neutrophils, *Nat. Cell Biol. 4*, 513−518.
45. Bode, A. M., and Dong, Z. (2003) Mitogen-activated protein kinase activation in UV-induced signal transduction, *Science 167*, 1−15.
46. Klotz, L. O., Pellieux, C., Briviba, K., Pierlot, C., Aubry, J. M., and Sies, H. (1999) Mitogen-activated protein kinase (p38-, JNK-, ERK-) activation pattern induced by extracellular and intracellular singlet oxygen and UVA, *Eur. J. Biochem. 260*, 917−922.
47. Kabuyama, Y., Hamaya, M., and Homma, Y. (1998) Wavelength specific activation of PI 3-kinase by UVB irradiation, *FEBS Lett. 441*, 297−301.
48. Zhang, Y., Dong, Z., Nomura, M., Zhong, S., Chen, N., Bode, A. M., and Dong, Z. (2001) Signal transduction pathways involved in phosphorylation and activation of p70S6K following exposure to UVA irradiation, *J. Biol. Chem. 276*, 20913−20923.
49. Schwarze, S. R., Hruska, K. A., and Dowdy, S. F. (2000) Protein transduction: Unrestricted delivery into all cells? *Trends Cell Biol. 10*, 290−295.
50. Ho, A., Schwarze, S. R., Mermelstein, S. J., Waksman, G., and Dowdy, S. F. (2001) Synthetic protein transduction domains: Enhanced transduction potential in vitro and in vivo, *Cancer Res. 61*, 474−477.
51. Deutscher, M. P. (1990) Guide to Protein Purification, *Methods Enzymol. 182*, 239−282.
52. Lee, C. L., Linton, J., Soughayer, J. S., Sims, C. E., and Allbritton, N. L. (1999) Localized Measurement of Kinase Activation in Oocytes of *Xenopus laevis*, *Nat. Biotechnol. 17*, 759−762.
53. Schafer, F. Q., and Buettner, G. R. (2001) Redox environment of the cell as viewed through the redox state of the glutathione disulfide/glutathione couple, *Free Radical Biol. Med. 30*, 1191−1212.
54. Levy, E. J., Anderson, M. E., and Meister, A. (1993) Transport of glutathione diethyl ester into human cells, *Proc. Natl. Acad. Sci. U.S.A. 90*, 9171−9175.
55. Holmes, C. P. (1997) Model Studies for New *o*-Nitrobenzyl Photolabile Linkers: Substituent Effects on the Rates of Photochemical Cleavage, *J. Org. Chem. 62*, 2370−2380.
56. Lundberg, M., and Johansson, M. (2002) Positively charged DNA-binding proteins cause apparent cell membrane translocation, *Biochem. Biophys. Res. Commun. 291*, 367−371.
57. Scheller, A., Wiesner, B., Melzig, M., Bienert, M., and Oehlke, J. (2000) Evidence for an amphipathicity independent cellular uptake of amphipathic cell-penetrating peptides, *Eur. J. Biochem. 267*, 6043−6050.
58. Console, S., Marty, C., Garcia-Echeverria, C., Schwendener, R., and Ballmer-Hofer, K. (2003) Antennapedia and HIV transactivator of transcription (TAT) "protein transduction domains" promote endocytosis of high molecular weight cargo upon binding to cell surface glycosaminoglycans, *J. Biol. Chem. 278*, 35109−35114.
59. Soughayer, J. S., Krasieva, T., Jacobson, S. C., Ramsey, J. M., Tromberg, B. J., and Allbritton, N. L. (2000) Characterization of cellular optoporation with distance, *Anal. Chem. 72*, 1342−1347.
60. Togo, T., Alderton, J. M., Bi, G. Q., and Steinhardt, R. A. (1999) The mechanism of facilitated cell membrane resealing, *J. Cell Sci. 112*, 719−731.
61. McNeil, P. L., and Steinhardt, R. A. (1997) Loss, restoration, and maintenance of plasma membrane integrity, *J. Cell Biol. 137*, 1−4.

BI036296D